American Journal of Sciences and Engineering Research
E-ISSN -2348 – 703X, Volume 5, Issue 2, 2022

Performance Estimation of the Wave Energy Recovery System on the East Coast of Madagascar

Andriantsitoha Romuald ROGER[1], Ruffin MANASINA [2], Nirilanto M. RASOLOZAKA[1], Jean Marc RABEHARISOA[1], Lucius RAMIFIDISOA[3], Adolphe A. RATIARISON [1]

[1]*Atmosphere, Climate and Oceans Dynamics Laboratory (DyACO), Physique and Applications, Sciences and technologies University of Antananarivo, Madagascar*
[2]*Higher Institute of Science and Technologies of Mahajanga (ISSTM), Madagascar*
[3]*Mathematics Laboratory and Computer Science ENSET, University of Antsiranana Madagascar*

ABSTRACT : *The development of wave energy recovery devices requires an in-depth knowledge of the site topology and sea states. The objective of this paper is to study the wave behaviour in the East coast of Madagascar, which allows to estimate the performance of the wave systems. The Kohonen network was used to regionalize the area of study according to the wave parameter characterisations. The ECMWF reanalysis data between 01st January 2015 and 31st December 2020 was used. The results show that the area of study is subdivided into three sub-areas named zone 1, zone 2 and zone 3 influenced mainly by the mean period, significant wave height and direction. Period of zones 1, 2 and 3 are characterised respectively as low, medium and high period. Zone 1 and 3 touch the East coast of Madagascar. Significant height wave are low or high. Direction of wave propagations in zone 1, zone 2 and zone 3 are respectively ESE, SE and SSE. The occurrence of the parameters varies from 16.7% to 83.3% (with maximum period of 10.5 s and maximum significant height of 3.1 m, from SSE 179°) whatever the area and the season. The average annual recoverable powers is 27.76kW/m for zone 1 and 27.76 kW/m for zone 3. These different powers allow to consider a new and reliable concept of wave energy recovery in this area.)*

Key words : *Wave energy, Wave power system, East coast of Madagascar, Wave parameters, Kohonen network.*

I. INTRODUCTION

Renewable energies are primary energies that are inexhaustible on a human scale [1]. They are the direct result of regular or constant natural phenomena linked to the energy of the sun and gravitation. According to the World Energy Council, the global energy potential of wave energy is estimated between 8,000 and 80,000 TWh/year [2][3][4]. In Madagascar, the annual average of the wave front power per metre is in the order of 10 to 50 kW/m) [5]. The characteristic and potential of the adapted wave system on the coastal structure is estimated by the on-site wave data [6], [7]. For some years, studies have been conducted to optimise wave energy recovery systems. For example, Neuvéglise is initiating its study of the behaviour of a shore-based float by analysing sea state data from the Esquibien site. More than 50% of mean energy period and significant wave height are between 5 s and 7 s and 0.5 m and 2 m respectively [4]. In a similar way, Michard et al. [7] carried out the analysis and dimensioning of the energy production of the oscillating wave system in the framework of the EMACOP project. The maximum energy is recovered for swells with a period between 9 s and 11 s and a significant height between 0.5 m and 1.5 m. In addition, most of the energy is recovered in the winter season than in the summer. More recently, Baudry et al. showed that the optimal power produced by the inverted beater system is 359.57 MWh/year, for the couple height-period (2 m, 12 s) [8]. This paper aims to study wave behaviour in order to estimate the performance of coastal wave systems in the East of Madagascar. We performed Kohonen regionalization of our study area and statistical analysis of the three wave parameters, namely mean period, significant height, and mean direction. Results show that the power obtained will make it possible to propose a more favorable concept for the recovery of wave energy.)

II. MATERIALS AND METHODS

2. 1- Presentation of the study area and datasets

The study area is located in the coastal and maritime regions of the East part of Madagascar covering an area of approximately 1,280,000 km^2 , shown in Figure 1. It is located between latitude 16.5°S to 29.5°S and longitude 45°E and 55°E, characterised by 437 grid points. Its climate is almost tropical, with two seasons: a dry season from May to October and a rainy season from November to April. Two short off-seasons with a duration of about one month each separate these two seasons. In this study, data on the significant height, mean period, and mean direction of wave propagations from 01st January 2015 to 31st December 2020 are obtained from the *European Centre Medium-Range Weather Forecasts (ECMWF) ERA5 (ECMWF Reanalysis 5th Generation)* so-called Copernicus. These data have a high spatial resolution of 30 km and are measured at 6-hour time steps over a 6-year period, with a NetCDF *(Network Common Data Form)* extension.)

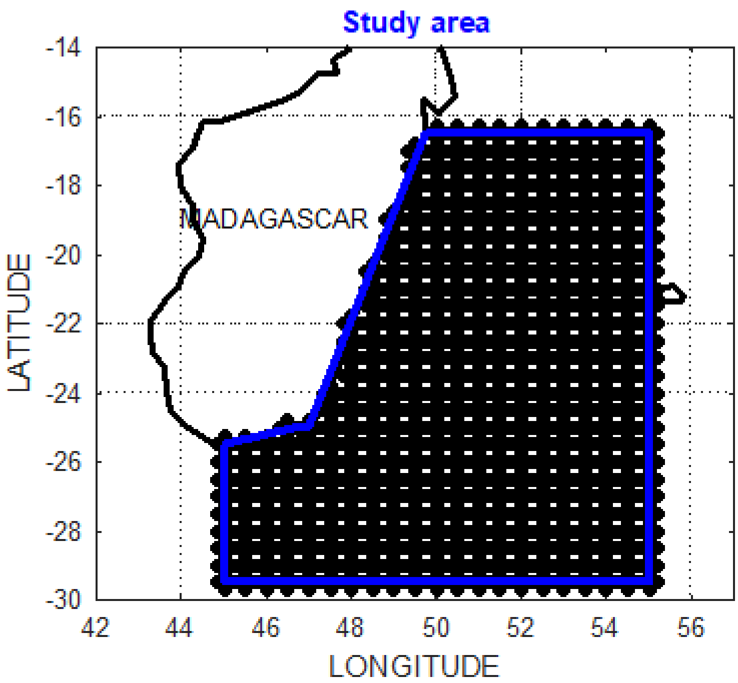

Figure 1: Location map of the study area, boxed in blue (lat.: 16.5°S to 29.5°S, long.: 45°E to 55°E)

2. 2- Methodologies

2.2.1- Kohonen's self-organising map

The neurobiologically inspired Self-Organising Map [10], [11], also known as Kohonen's network [12], [13] is a method belonging to the field of artificial intelligence. It is proving to be a very powerful tool for data analysis. The Kohonen network is a type of unsupervised network based on competitive learning[14] and has the concept of classifying training vectors into groups, each represented by an output neuron. The aim of this type of classification is to increase the inter-class distances and reduce the intra-class distances, so that the elements of a class are more similar to each other. To create this map, we will first choose the type of classification according to the size of the map whose optimal dimension is given by the relation : $M \times 5 \times (N)^{1/2}$ where M is the number of neurons in a map and N is the number of observations.

2.2.2- Kohonen's Self-Organizing Map Algorithm

Table 1 shows the Self-Organizing Map (SOM) algorithm, with $R(t)$: Neighbourhood radius of the neuron defined beforehand , L et K : Number of Columns and Rows , $\alpha(t)$: learning rate, $(0 \le \alpha \le 1)$, $\vec{X}$: Input vector, D : Grid diameter (With $D = (L+K)/2$), $\mu_{i,D}$: Coefficient with index i and D, C : Identity of the winning neuron, $h_{C,i(t)}$: Neighbourhood rate at index $C, i(t)$ and $\overrightarrow{w_i}$: Poids.

Tableau 1 : Table 1: Kohonen's Self-Organizing Map Algorithm [15]

Initialization :		
		1. Initialise the weight vectors of each neuron.
		2. Initialise the learning parameters.
		$t = 0;\ R(0) = \text{major}\left(\frac{(K+L)}{2}\right); \alpha(0) \Box 1$ (1)
Training :		
	- Competition:	3. Randomly select a sample from the training base.
		4. Present the input vector $\vec{X}$ on the input layer).
		$\vec{X} = (\xi_1, \xi_2, \dots, \xi_D) \in Re^D$ (2)
		5. Calculate the Euclidean distance for each neuron.
		$\left\Vert \vec{X}\ \vec{W_i} \right\Vert = \sqrt{(\xi_1\ \mu_{i,1})^2 + (\xi_2\ \mu_{i,2})^2 + \dots + (\xi_D\ \mu_{i,D})^2}$ (3)
		6. Search for the identity of the winning neuron.
		$C = \arg\min = \left\Vert \vec{X}\ \vec{W_i} \right\Vert$ (4)
	- Adaptation :	7. Calculating the neighbourhood rate
		$h_{C,i(t)} = \exp\left(\frac{\vec{r_c}\ \vec{r_i}}{2\sigma^2(t)}\right)$ (5)
		8. Update the weight vector (6)
		$\overrightarrow{w_i}(t+1) = \begin{cases} \overrightarrow{w_i}(t) + \alpha(t) \times h_{C,i(t)} \times \left(\vec{X} - \overrightarrow{w_i}(t)\right) & \text{si} \left\Vert \vec{r_c} - \vec{r_i} \right\Vert \le R(t) \\ \overrightarrow{w_i}(t) & \text{else} \end{cases}$
		9. Update the learning parameters.
		$t = t+1; \alpha(t+1) = \alpha(t) - \frac{t}{500 \times L \times K}$ (7)
		$R(t+1) = R(t) - \text{major}\frac{t}{50 \times L \times K}$ (8)
Reminder:		
	- Competition :	10. Present a vector $\vec{X}$ of real space on the input layer.
		11. Calculate the Euclidean distance for each neuron.
		12. Search for the identity of the winning neuron.
	- Decision :	13. Identify the class of the vector on the output layer cluster.

2.2.3- Wave energy resources

Due to the random nature of waves, the sea state is described by statistical parameters, such as the significant height and the average energy period [16]. In this study area, the intensity of gravity and the density of seawater are 9,79 kg/N and 1025 m^3 /kg respectively. In order to consider the phenomenon of the superposition of several waves, the average power per metre of wave front in the direction of propagation is obtained according to equation (9) and (10)[18], [19].

$$P_w = 500 \times {H_s}^2 \times Te \left(W/m\right) \quad (9)$$

In kilowatts per metre we get :

$$P_{kW} = (1/2) \times {H_s}^2 \times Te \ \left(kW/m\right) \quad (10)$$

where Hs is the significant wave height and Te is the wave energy period.

III. RESULTS AND DISCUSSION

3.1- Presentation of daily reanalysis data

Figure 2 and Figure 3 show respectively the spatial distribution of annual mean significant wave height and mean energy period in the East of Madagascar for six years (from 2015 to 2020).

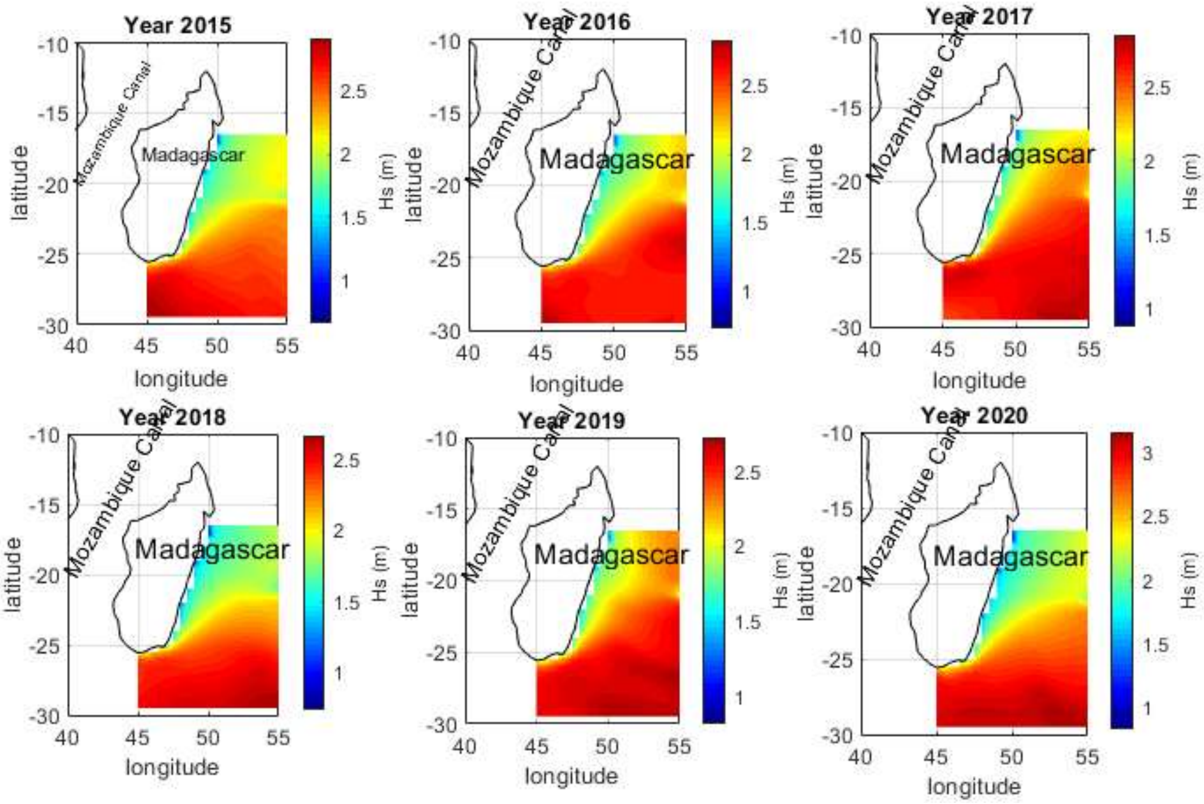

Figure 2: Annual average significant wave height from 2015 to 2020

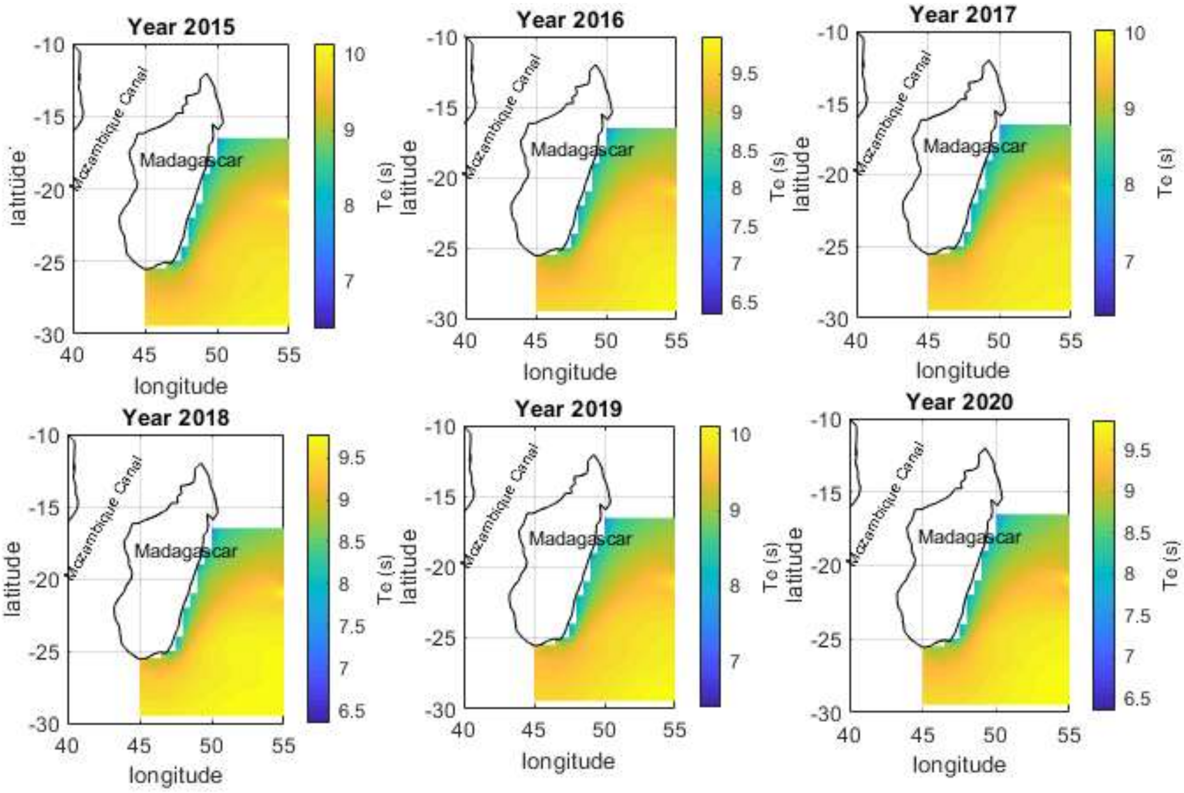

Figure 3: Annual average wave period from 2015 to 2020

3.2- Regionalization of wave parameters)

The neural map contains 6 x 7, which makes 42 neurons in the map sufficient for each of these parameters. The quality of the classification depends on the convergence of the learning progress: the intra-class distance should be as small as possible. The learning progress for the classification of the mean period, direction and significant wave height converges after 2000 iterations. Learning stop after 2500 iterations. For each of the parameters, at the end of the convergence, the numbers of individuals gained by each neuron are plotted and represented on the neuron map. The maps contain only one empty neuron out of 42 for the mean period parameter, two out of 42 for the significant height and three out of 42 for the mean wave direction.)

3.2.1- Map of classified neurons

The Kohonen self-organising map used for the three parameters (Mean period, Significant height and Mean wave direction) contains 42 neurons (6x7) grouped in three classes or clusters as shown in Mapping plot (figure 4). The closest neurons are thus grouped together to form the three distinct classes: class 1, class 2 and class 3

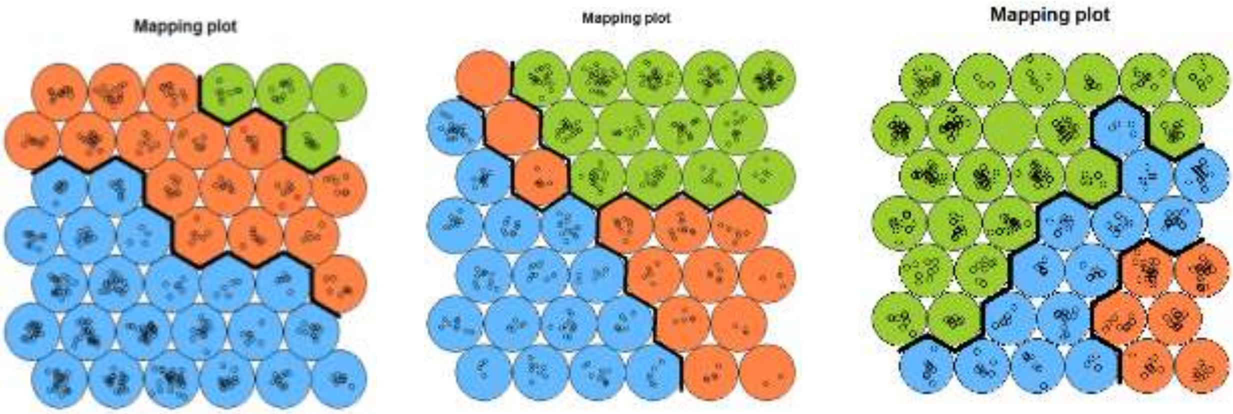

(a) Mean wave period (b) Significant wave heights (c) Mean wave direction

Figure 4: Map of classified wave parameter neurons

The characteristics of the neurons, their indexes and classes are defined from the interconnection distance and according to their class, they are given in Table 2. The neurons are numbered from left to right and from bottom to top; neuron 1 is at the lower left and neuron 42 at the upper right and the classification of the neurons are given in Table 2.

Table 2: Classification of neurons (by index)

CLASS / a) -Te	Neuron indexes
Classe 1 (Green)	36, 40, 41, 42
Classe 2 (Red))	18, 22, 23, 24, 27, 28, 29, 30, 31, 32, 33, 34, 35, 37, 38, 39
Classe 3 (Blue))	1, 2, 3, 4, 5, 6, 7, 8, 9, 10, 11, 12, 13, 14, 15, 16, 17, 19, 20, 21, 25, 26

CLASS / b) - Hs	Neuron indexes
Classe 1 (Green)	27, 28, 29, 30, 33, 34, 35, 36, 38, 39,40, 41, 42
Classe 2 (Red)	5, 6, 11, 12, 16, 17, 18, 22, 23, 24, 26, 32, 37
Classe 3 (Blue)	1, 2, 3, 4, 5, 6, 7, 8, 9, 10, 13, 14, 15, 19, 20, 21, 25, 31

CLASS / c) - Dir	Neuron indexes
Classe 1 (Red)	5, 6, 11, 12, 17, 18
Classe 2 (Blue)	1, 2, 3, 4, 9, 10, 15, 16, 22, 23, 24, 29, 30, 35
Classe 3 (Green)	7, 8, 13, 14, 19, 20, 21, 25, 26, 27, 28, 31, 32, 33, 34, 36, 37, 38, 39, 40, 41, 42

3.2.2- Code plot of data distribution

The neural map represents the character of the month variables for the whole year and is shown in Figures 5 and 6. It can be seen that neuron number 42 has individuals with low wave periods in all months of the year and neuron number 1 has individuals with higher mean wave periods. For significant height, the distribution is reversed.

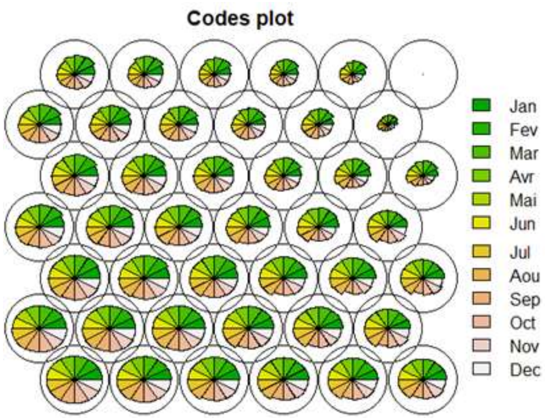

Figure 5: Codes plot of the mean wave period data distribution for each month

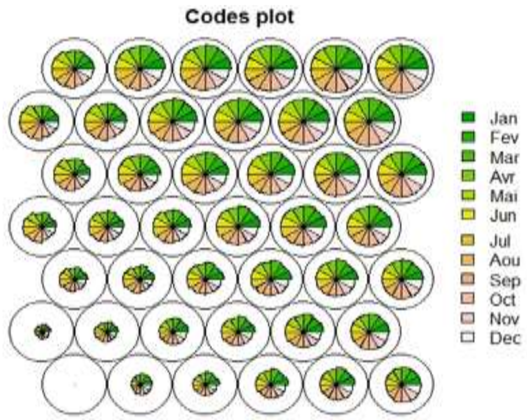

Figure 6: Codes figure of the distribution of significant wave height data for each month.

3.2.3- Histogram of the classification of the different parameters

The histogram in Figure 7-a represents the classes of the mean wave period in our study area while respecting the classification and while checking the distribution of variables in Figure 5.

The green area (class 1) has the lowest period value, the red area is medium, and the blue area has the highest value in all months of the year. Figure 7-b shows that the climatological monthly variation of the significant height. Class 3 (green) is much higher than class 2 (red) and class 1 (blue). Figure 7-c shows the mean direction of the wave origin from ESE115° class 1 to SSE179° class 3.

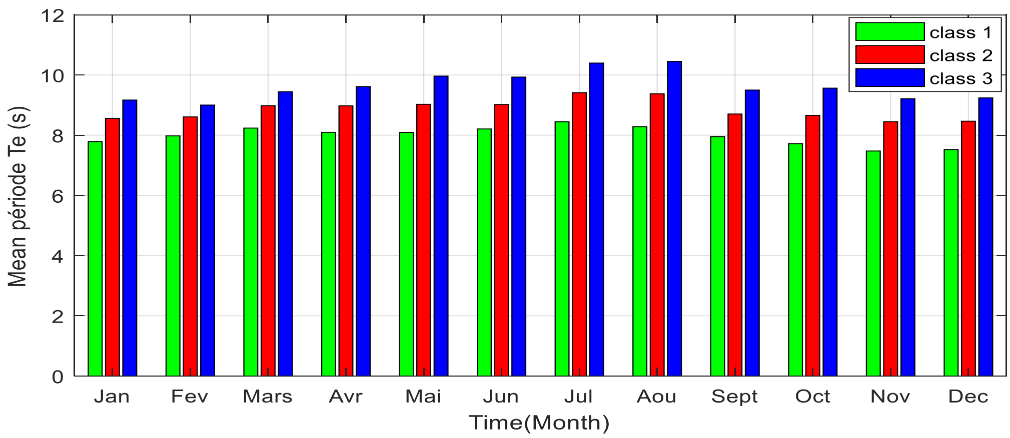

(a) Mean wave period

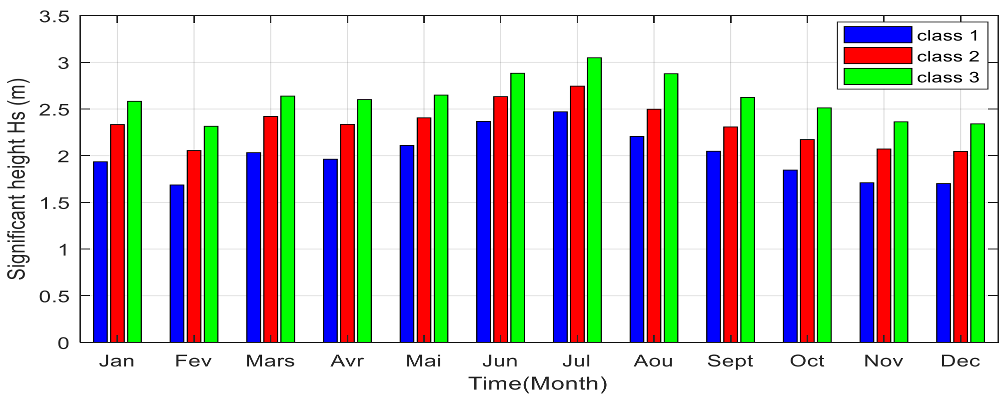

(b) Significant wave height

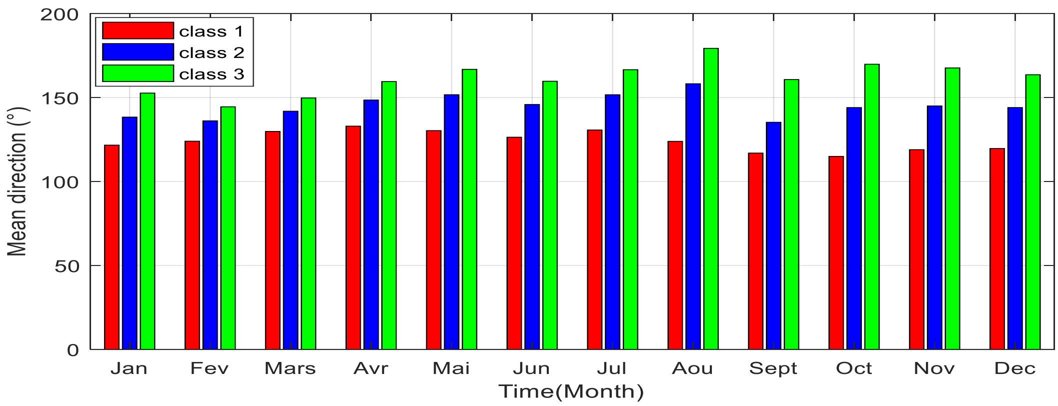

(c) Mean wave direction

Figure 7: Histogram of the monthly climatological mean wave parameters for the 3 classes

3.2.4- Mapping of data classification in the study area

The classification of the different wave parameters is shown on the geographical map (Figure 8 : Figure 8-a, Figure 8-b and Figure 8-c).

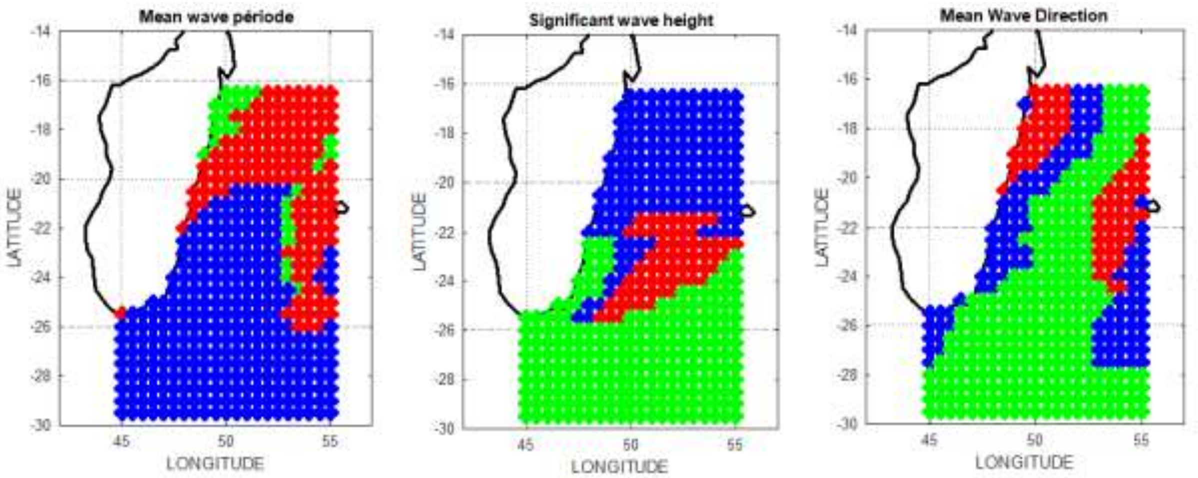

(a) Mean period zone 1 (**Green**), zone 2 (Red) and zone 3 (**Blue**)

(b) Significant height zone 1 (**Green**), zone 2 (Red) and zone 3 (**Blue**)

(c) Mean wave direction zone 1 (Red), zone 2 (**Blue**) and zone 3 (**Green**)

Figure 8: Map representation of the data classification

3.3- Occurrence frequency of wave parameters

The percentages of occurrences for all three classes are presented as follows :

3.3.1- Frequency of occurrence for the Mean wave Period

Class 1 : Te varie from 8 s to 8.5 for the maximum frequency of 41.98%

Class 2 : Te varie from 8.5 s to 9 s for the maximum frequency of 48.31 %

Class 3 : Te varie from 9 s to 9.5 s for the maximum frequency of 38.17 %

3.3.2- Occurrence frequency of significant height

Class 1 : Hs varie from 1.5 to 2 m for the maximum frequency of 45.50 %

Class 2 : Hs varie from 2 to 2.5 m for the maximum frequency of 69.67 %

Class 3 : Hs varie from 2.5 to 3 m for the maximum frequency of 61.94 %

3.3.3- Occurrence frequency of the mean wave direction

Occurrence frequency of the wave direction is presented by a wind rose diagram (Figure 9).

Class 1 : Hs varie from 2.2 à 2.3 m, the maximum frequency is 40 %, of direction SE120°
Class 2 : Hs varie from 2.4 à 2.5 m, the maximum frequency is 40 %, of direction SSE160°
Class 3 : Hs varie from 3 à 3.1 m, the maximum frequency is 27.2 %, of direction SSE160°

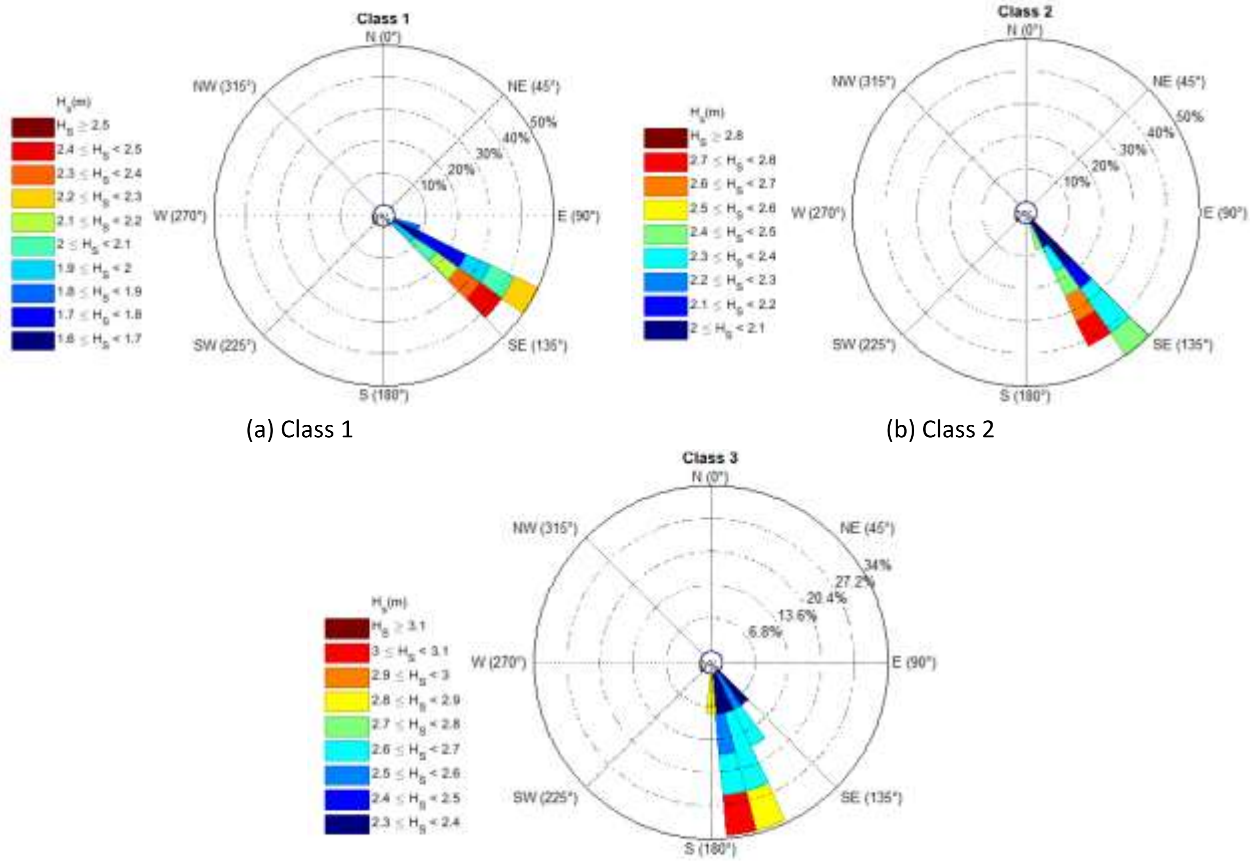

(a) Class 1 (b) Class 2

(c) Class 3

Figure 9: Rose of mean direction of wave origin over the year

3.4- Seasonal variation of wave parameters

3.4.1- Seasonal variation of the mean wave period

For each sub-zone (class) (Table 3-a, 3-b and 3-c), during the winter period, the mean wave period varies from 7.5 s to 10.5 s and in summer from 7.37 s to 9.61 s.

Table 3: Seasonal distribution of mean wave period

a) - Sub-zone						
Season	**Te mean (s)**	**[6-6.5]**	**[6.5-7]**	**[7-7.5]**	**[7.5-8]**	**[8-8.5]**
Winter	Percentage (%)	0	0	0	33.33	66.66
Summer	Percentage (%)	0	0	16.66	50	33.33
b) - sub-zone 2						
Season	**Te mean (s)**	**[7-7.5]**	**[7.5-8]**	**[8-8.5]**	**[8.5-9]**	**[9-9.5]**
Winter	Percentage (%)	0	0	0	33.33	66.66
Summer	Percentage (%)	0	0	33.33	66.66	0
c)- Sub-zone 3						
Season	**Te mean (s)**	**[8-8.5]**	**[8.5-9]**	**[9-9.5]**	**[9.5-10]**	**[10-10.5]**

Winter	Percentage (%)	0	0	16.66	50	33.33
Summer	Percentage (%)	0	0	83.33	16.66	0

3.4.2- Seasonal variation in significant wave height

The frequency distributions of significant wave height during summer and winter are shown in Table 4.

Sub-zone 1: During the winter period, 83% of the waves have heights between 2 m and 2.5 m. In summer, only 16.66 % of the wave height is between 2 m and 2.5 m.

Sub-zone 2 : During winter, 50% of the waves have heights between 2 m and 2.5 m and 33.33% between 2.5 m and 3 m. In summer, the height is between 2 m and 2.5 m.

Sub-zone 3 : During winter, 16.66 % of the waves have heights between 3 m and 3.5 m and 83.33 % between 2.5 m and 3 m. In summer, 50% of the frequency of occurrence of waves between 2 m and 2.5 m high and 50% between 2.5 m and 3 m.)

Table 4: Seasonal distribution of significant wave height

a) - Sub-zone 1

Season	Hs (m)	[0.6-1]	[1-1.5]	[1.5-2]	[2-2.5]	[2.5-3]	[3-3.5]
Winter	Percentage (%)	0	0	16.66	83.33	0	0
Summer	Percentage (%)	0	0	83.33	16.66	0	0

b) - Sub-zone 2

Season	Hs (m)	[0.6-1]	[1-1.5]	[1.5-2]	[2-2.5]	[2.5-3]	[3-3.5]
Winter	Percentage (%)	0	0	16.66	50	33.33	0
Summer	Percentage (%)	0	0	0	100	0	0

c)- Sub-zone 3

Season	Hs (m)	[0.6-1]	[1-1.5]	[1.5-2]	[2-2.5]	[2.5-3]	[3-3.5]
Winter	Percentage (%)	0	0	0	0	83.33	16.66
Summer	Percentage (%)	0	0	0	50	50	0

3.5- Evaluation of wave energy powers

The powers per metre of wavefront are shown in Figure 10 according to their corresponding sub-zones.

Sub-zone 1, scatter sub-zone 1: According to Figure 10-a, the maximum energy (P_max) over time is recovered in July with P_max = 25.76 kW/m. The corresponding wave period is Te = 8.441 s with a height Hs = 2.47 m.

Sub-zone 2, Sub-zone 2, scatter sub-zone 2:In Figure 10-b, the peak available power (P_max) is reached in July of P_max = 35.45 kW/m for a height Hs =2.745 m and a period Te = 9.41 s.

Sub-zone 3, scatter sub-zone 3: Figure 10-c shows that the maximum power available is 48.32 kW/m in July. It corresponds to the significant height Hs = 3.049 m and the period Te = 10.4 s.

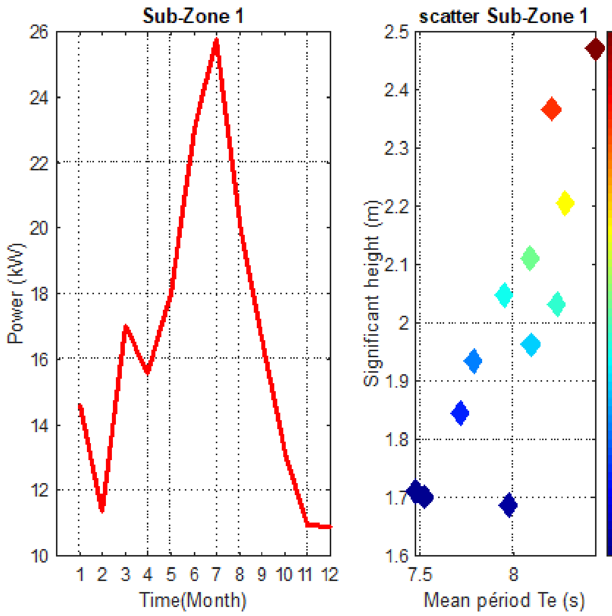

(a) Sub-zone 1

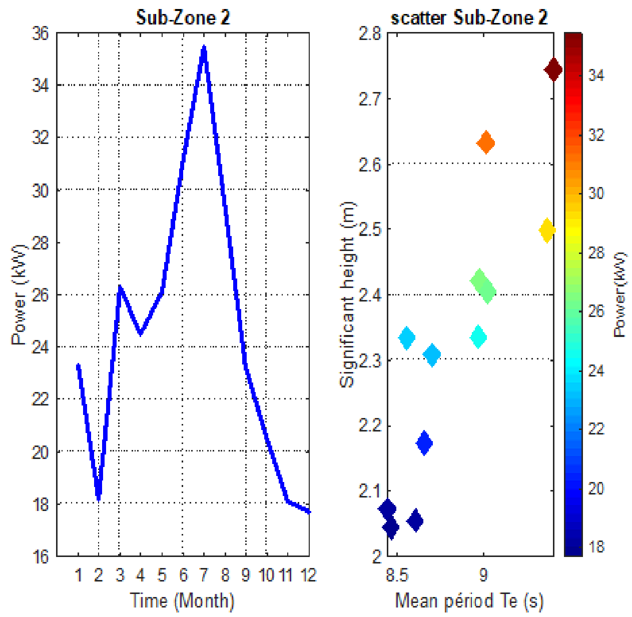

(b) Sub-zone 2

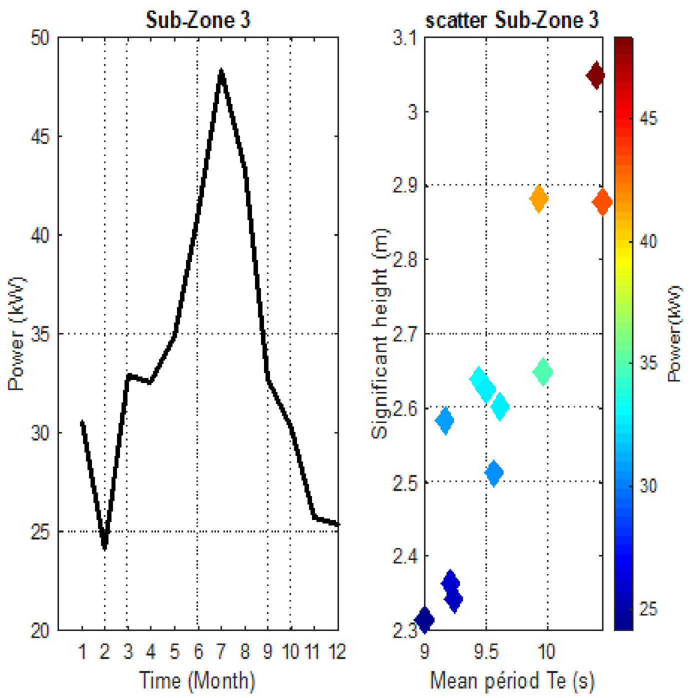

(c) Sub-zone 3

Figure 10 : Wave energy levels in the sub-zones (kW/m)

3.6 - Discussion of the Kohonen Network Method

The Principal Component Analysis (PCA) and the kohonen network are two methods that can be used for data analysis and classification. For our study, we chose to perform the classification of the characteristic wave parameters on the East part of Madagascar using the Kohonen network method. This method allowed to obtain three sub-zones (sub-zone 1, sub-zone 2, sub-zone 3). The choice of this method is in line with the results of the work of Rasolozaka et al [20]. A better classification of the parameters allows to have a more reliable estimate of the performance of wave energy recovery system in our zone. This makes classification a crucial step in the study of wave energy recovery system performance estimation.

IV. CONCLUSION

In this study, we used the Kohonen network regionalization method to get a better estimate of the performance of the wave system. This method allowed to subdivide the study area into three areas according to the wave behaviour. In sub-zone 1, the period and significant height are low and the mean direction is East-South-East. The mean significant height, mean period and direction of South-East waves are grouped in sub-zone 2. High values of period and height are collected in sub-zone 3. The wave directions in this sub-area are South-South-East. For a maximum period-height pair (Te, Hs), the estimated power is 48.32 kW/m (10.40 s, 3.05 m) in zone 3, 35.45 kW/m (9.41 s, 2.75 m) in zone 2, and 25.76 kW/m (8.40 s, 2.47 m) in zone 1. Therefore, the mean wave period, significant wave height and mean wave direction in the East coast of Madagascar are favourable for coastal energy development. Following this classification in terms of energy potential, we plan to design and optimise a wave energy recovery system using a venturi flow.

V. REFERENCES

[1] A. Miloud et A. Lyes, Etude et maximisation d'un système éolien, République Algérienne Démocratique et Populaire: Mémoire de fin d'étude, 2013.

[2] A. W. Clarke et J. Trinnaman, 2010 Survey of Energy Resources, London W1B 5LT United Kingdom: World Energy Council, 2010.

[3] A. W. Clarke et J. Trinnaman, 2004 Survey of Energy Resources, London W1B 5LT United Kingdom: World Energy Council, 2004.

[4] N. Sixtine, Modélisation numérique et physique de la chaîne de récupération de l'énergie de la houle par un dispositif bord à quai, Normandie: Normandie Université, 2018.

[5] K. Gunn et S. W. Clym, «Quantifying the global wave power resource,» SciVerse ScienceDirect, vol. 44, n° ISSN 0960-1481, pp. 296-304, 2012.

[6] N. Sixtine , P. Gaële , S. Hassan , M. François et S. Philippe , «Two-Dimensional Modelling of a Quayside Floating System,» Marine Sience and Engineering, vol. 8, n° 908, pp. 1-10, 2020.

[7] B. MICHARD, S. BOULAND, P. SERGENT, S. NEUVEGLISE et V. BAUDRY, «Projet EMACOP : analyse économique de la production d'énergie renouvelable de systèmes houlomoteurs sur le site d'Esquibien (Finistère),» La Rochelle, pp. 543-554, 2018.

[8] V. Baudry, A. Babarit et A. Clément, «An overview of analytical, numerical and experimental methods for modelling oscillating water columns,» Hal, pp. 1-10, 2019.

[9] R. Zoaharimalala , A. L. Y. Randriamarolaza et M. L. Rakotondrafara, Le changement climatique à Madagascar, Antananarivo: Direction Générale de la Météorologie, 2009.

[10] A. Umut et E. Secil , «An Introduction to Self-Organizing Maps,» Computational Intelligence Systems in Industrial Engineering, pp. 299-319, 2012.

[11] A. P. Engelbrecht, Computational Intelligence, 2e éd., Pretoria, South Africa: John Wiley & Sons, 2007.

[12] T. Kohonen, «Self-Organized Formation of Topologically Correct Feature Maps,» Biological Cybernetics, n° 43, pp. 59-69, 1982.

[13] T. Kohonen, Self-Organizing Maps, 3e éd., New York: Springer, 2001.

[14] A. Richardson, C. Risien et F. Shillington, «Using self-organizing maps to identify patterns in satellite imagery,» Progress in Oceanography, n° 59, pp. 223-239, 2003.

[15] M. Abadi, Réalisation d'un réseau de neurones "SOM" sur une architecture matérielle adaptable et extensible à base de réseaux sur puce "NoC", Lorraine: Université de Lorraine, 2018.

[16] M. Houekpoheha, B. Kounouhewa, J. Hounsou, B. Tokpohozin et C. Awanou, «Analyse statistique des hauteurs de la houle sur la côte du Bénin dans le Golfe de Guinée: Puissance énergétique de la houle non-linéaire dans la zone de shoaling,» Revue des Energies Renouvelables, vol. 18, n° 1, p. 89 – 103, 20015.

[17] J. C. Ascione et P. Gaufrès, «Modélisation des états de mer pour la recherche de sites d'exploitation houlomotrice Application à l'île de la Réunion,» IXèmes Journées Nationales Génie Civil – Génie Côtier, pp. 13-20, 12-14 septembre 2006 , Brest.

[18] M. RUELLAN, Méthodologie de dimensionnement d'un système de récupération de l'énergie des vagues, Cachan: École normale supérieure de Cachan, 2007.

[19] E. R. Hanitra, Caracteristiques de la houle au large de la cote Est de Madagascar, Université Tananarivo: Laboratoire de Dynamique de l'Atmosphère, du Climat et des Océans (DyACO), 2018.

[20] N. RASOLOZAKA, N. A. RAKOTOVAO, J. M. RABEHARISOA et A. RATIARISON, «Regionalization of the precipitation Regime in the South Eastern Part of Madagascar,» IJARIIE-ISSN(O)-2395-4396, vol. 5, pp. 566-576, 2019.